

Electronic Properties of Nonstoichiometric PbSe Quantum Dots from First Principles

Yanqin Gai,^{†,‡} Haowei Peng,[†] and Jingbo Li^{*,†}

State Key Laboratory for Superlattices and Microstructures, Institute of Semiconductors, Chinese Academy of Sciences, P.O. Box 912, Beijing 100083, and Department of Physics, School of Sciences, China University of Mining and Technology, Xuzhou 221008, People's Republic of China

Received: June 23, 2009; Revised Manuscript Received: November 06, 2009

The electronic properties of PbSe quantum dots containing a nonstoichiometric Pb:Se ratio are investigated by ab initio density functional theory. We take five nearly spherical PbSe nanocrystals with effective diameters ranging from 11.22 to 31.86 Å into account and compare their electronic properties before and after passivations. We find that despite the strong ionic character of the Pb–Se bond, their dangling bonds at the surface of *nonstoichiometric* PbSe nanocrystals introduce in-gap states, which are quite different from those of the *stoichiometric* PbSe nanocrystals. The same phenomenon is also observed for bare PbSe (011) and (111) surfaces. Compared with that of the self-passivated (001) surface, there is large surface relaxation and rumpling at the unsaturated (011) and (111) surfaces. We expect this might also be the origin of surface states in nonstoichiometric PbSe nanocrystals. We observed the almost recovery of structures and at the same time the elimination of in-gap states by passivating the dangling bonds with pseudo-hydrogen atoms. Meanwhile, the size dependencies of the QDs' gaps are obtained, which are in accordance with experimental measurement and other theoretical calculations.

I. Introduction

The narrow bulk band gap (~0.28 eV at 300 K)¹ and strong quantum confinements (exciton Bohr radius ~46 nm)² render PbSe quantum dots (QDs), one of the most promising building blocks in nanotechnology applications, especially in the fabrication of highly efficient solar cells.^{3–7} Knowledge of the nanocrystals' electronic structures is required for the interpretation of experimental observations. Up to now, a number of theoretical approaches have been employed to investigate the electronic properties of PbSe QDs. These include the $k\cdot p$ Hamiltonian,^{7–9} empirical tight-binding (TB) approximation,^{10,11} and atomistic pseudopotential approach.¹² However, almost none of these models can consistently explain all of the experimentally observed features of PbSe QDs, as all of them are highly approximated in nature.^{13–15} For example, for PbSe nanocrystals, the $k\cdot p$ approximation does not include the multiple valleys located along the $L-K$ and $K-X$ lines. Lately, the predicated “mirror symmetry” between the valence band and conduction band by $8 \times 8 k\cdot p$ is proven to be not present by pseudopotential and first-principles calculations.¹⁶ Besides, it exaggerates the degree of quantum confinement, because this is applied by using an infinite potential barrier. The TB calculations missed the anisotropy of the L -valley. Since the strong anisotropy of the L -valley can further split the near-edge states, the optical properties of PbSe QDs cannot be fully predicted by such a method. In addition, both the TB and the pseudopotential methods have uncertainty in their fitting parameters. Consequently, it is desirable to perform much more reliable first-principles calculations, which have been successfully applied to the investigations of Si QDs,¹⁷ II–VI and III–V QDs,¹⁸ and even some core/shell QDs,¹⁹ etc.

Recently, the atomic and electronic structures of *stoichiometric* (with Pb:Se = 1:1) PbSe QDs have been investigated by Franceschetti¹⁶ using first-principles calculations. The author concluded that the stoichiometric PbSe QDs are free from gap states even in the absence of surface passivation. The author also pointed out in his work that, for *nonstoichiometric* PbSe QDs, dangling bonds at the surfaces would create a large density of surface states inside the band gap. However, no detailed discussions regarding the origin of them are given. For example, the author does not study the PbSe (011) and (111) surfaces, which are very important for nonstoichiometric PbSe QDs. Our present work represents a *further* study of composition dependence (Pb-rich or Se-rich) of the electronic properties of PbSe QDs, as in actual experiments the usually obtained PbSe QDs are nonstoichiometric ones.²⁰ Brumer and Sashchiuk et al. have shown that the luminescence quantum efficiencies in PbSe/PbS core/shell structures could be substantially increased, due to the efficient chemical passivation of the PbSe core with PbS.^{21,22} Their works indirectly prove the presence of surface states in bare PbSe nanocrystals. For nanosystems, the most common issue is the surface passivation. As the size of the crystal particle decreases, the surface states play a vital role in controlling the properties, especially the optical ones. Thus, reducing the influence of surface states on the QD properties is valuable for determining the intrinsic QD properties. In experiments, large organic molecules with complicated atomic details are usually employed to passivate the quantum dot surface. However, their complexes have impeded the employment of first-principles methods to study such systems. An et al. have employed the ligand potentials of a Gaussian form to passivate the dangling bonds at the surface of PbSe QDs,²³ yet the “empirical” character of such a method makes it far from first principles. In our work, we choose the hydrogen-like pseudo-hydrogen atom, which has been widely used in thin-film calculations to passivate the unwanted back surface atoms.²⁴

* To whom correspondence should be addressed. E-mail: jqli@semi.ac.cn.

[†] Chinese Academy of Sciences.

[‡] China University of Mining and Technology.

TABLE 1: Components, Effective Diameters, and Calculated LDA Band Gaps of Five Nonstoichiometric PbSe QDs

QD	formula	<i>d</i> (Å)	<i>E_g</i> (eV)
1	Pb ₁₄ Se ₁₃ (^{5/3} H) ₃₀ (^{1/3} H) ₂₄	11.216	2.689
2	Pb ₃₈ Se ₄₃ (^{5/3} H) ₄₈ (^{1/3} H) ₇₈	16.174	1.748
3	Pb ₉₂ Se ₉₇ (^{5/3} H) ₁₂₆ (^{1/3} H) ₉₆	21.452	1.624
4	Pb ₁₁₆ Se ₁₃₅ (^{5/3} H) ₁₇₈ (^{1/3} H) ₁₉₂	23.580	1.331
5	Pb ₂₉₈ Se ₃₂₁ (^{5/3} H) ₁₉₈ (^{1/3} H) ₃₃₆	31.858	0.842

II. Method

Local density approximation (LDA) calculations are performed using the plane-wave code VASP,²⁵ where the frozen-core projector-augmented-wave (PAW) method is used to represent the electron and core interactions.²⁶ A plane-wave cutoff energy corresponding to a kinetic energy of 300 eV is used. The PbSe (001) and (011) surfaces are modeled by periodically repeated slabs both containing up to 12 Pb–Se layers and 1 10 Å thick vacuum layer. To display the quantum confinement effect more clearly, the (111) surface is simulated with a 12-atom slab including the passivation agent pseudo-hydrogen atoms.

We consider here five nonstoichiometric PbSe QDs as given in Table 1. The construction of these nearly spherical QDs is the same as those by J. M. An et al. and Peng et al.^{27,28} The effective diameter *d* is defined by the formula $d = (a^3(n_{\text{Pb}} + n_{\text{Se}})/32\pi)^{1/3}$, where *a* is the calculated lattice constant of bulk PbSe and *n_{Pb}* and *n_{Se}* are the number of Pb and Se atoms in the QDs, respectively. The effective diameters of the five dots studied here are listed in Table 1.

The Brillouin zone (BZ) of PbSe surfaces is sampled using a $4 \times 4 \times 1$ Monkhorst–Pack *k* grid.²⁹ Only the Γ point is used to sample the QDs, as all the points in the BZ are folded to this point for very large systems. Full atomic relaxation is performed for all QDs.

III. Results and Discussion

A. Bulk Rock-Salt PbSe. Before presenting the results for PbSe QDs, we discuss some basic features for *bulk* PbSe from our LDA calculations. The calculated band structure and atom-

projected density of states (PDOS) for bulk PbSe are shown in parts a and b, respectively, of Figure 1. We can see from Figure 1a that both the conduction band minimum (CBM) and the valence band maximum (VBM) occurred at the *L* points in the BZ. The same results are also obtained by Wei et al. calculated from the general-potential linearized augmented plane-wave (LAPW) method.³⁰ This can be explained by the fact that the Pb 6s band lies deep inside the valence band (indicated by the red line in Figure 1a) arising from relativistic effects.³¹ This unique feature also accounted for some unique properties of PbSe in nanostructures as listed in ref 32. The calculated band gap in our work is 0.101 eV, smaller than the experimental value of about 0.145 eV at low temperature.³³ The PDOS in Figure 1b indicated that the upper part of the valence band is formed primarily of the Se 4p orbital, while the bottom of the conduction band is formed mostly of the Pb 6p orbital. The valence electron configuration of the Pb atom employed in our calculations is $6s^26p^2$. However, as the 6s electrons lie deep below the VBM, only the two p electrons participate in the chemical bonding with surrounding Se atoms. Meanwhile, rock-salt-structure PbSe is an octahedrally coordinated crystal, which together with the above unique electronic properties distinguishes PbSe dramatically from the ordinary tetrahedrally coordinated zinc-blende or wurtzite II–VI semiconductors. For surface passivation, the choices of pseudo-hydrogen atoms (with fractional nuclear charge *Z* and corresponding fractional number of electrons) differ apparently from each other. For tetrahedrally coordinated ZnO or GaN, *Z* has been chosen to be 0.5, 1.5, 0.75, and 1.25 for O, Zn, N, and Ga atoms, respectively.³⁴ Nevertheless, in the octahedrally coordinated NaCl-structure PbSe, every Pb or Se atom is surrounded by six Se or Pb atoms. As discussed above, the Pb atom has two valence electrons and Se has six. To form an octahedrally coordinated crystal, every Pb atom provides 2/6 electron to each of its six bonds. To pair the 1/3 e in each Pb dangling bond, a passivating agent is needed to offer 5/3 additional electrons. Therefore, we chose ^{5/3}H and ^{1/3}H to saturate the Pb and Se dangling bonds on the surface of PbSe, respectively.

B. Surfaces of Bulk PbSe. Figure 2 gives the total DOS comparisons among the PbSe (001), (011), and (111) surfaces

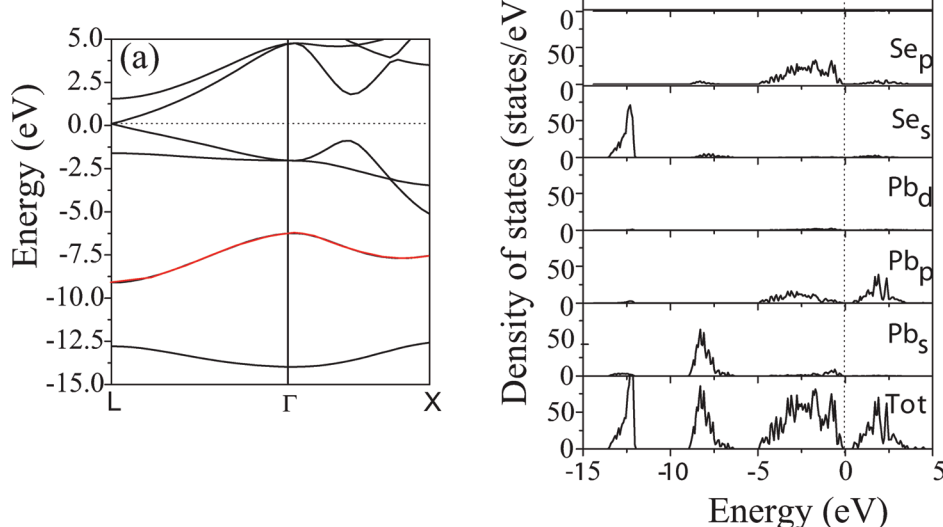


Figure 1. LDA-calculated band structure (a) and total and atom-projected densities of states (b) of bulk PbSe. The highest occupied state is chosen as the Fermi energy and is set to zero. The red line in (a) indicates the Pb 6s state.

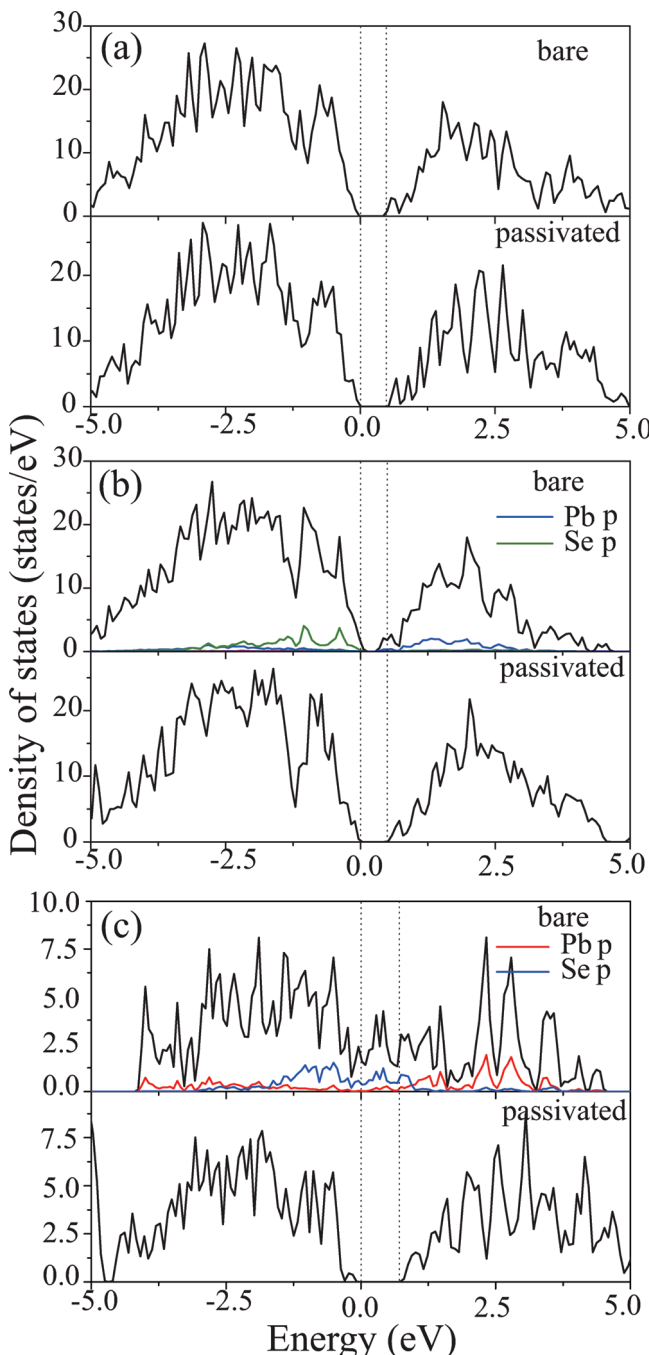


Figure 2. Total DOS comparisons among the PbSe (001) (a), (011) (b), and (111) (c) surfaces with and without passivations. The atom-projected density of states is also plotted for the Pb and Se atoms at bare surfaces. The zero energy corresponds to the highest occupied states.

before and after saturation by the corresponding pseudo-hydrogen atoms discussed in section A. As the (001) surfaces are the natural cleavage face of lead salts, a lot of theoretical and experimental works are conducted primarily on them.^{35–37} A general conclusion about it is that the dangling bonds at this surface would *not* introduce surface states inside the band gap even without passivation; that is, they are self-passivated. The same conclusion is also obtained in our present work as indicated in Figure 2a. The band gap for the (001) surfaces remains almost unchanged in the presence of saturation, which also means that our models of surfaces employed here are reasonable. However, for the bare (011) surface, we clearly see the presence of surface states below the conduction and above the valence band edges

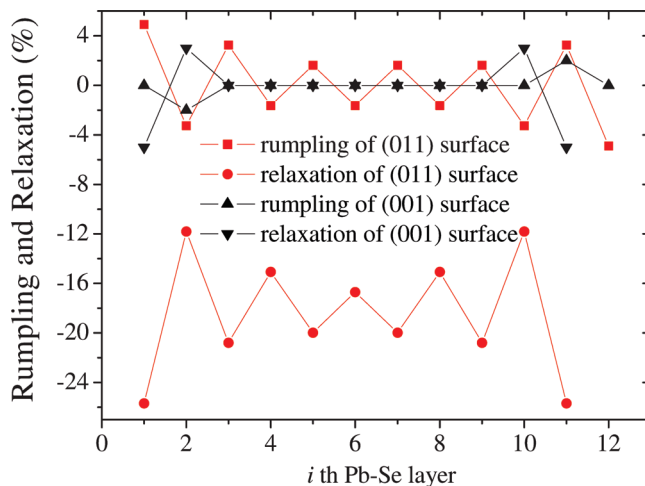


Figure 3. Layer rumpling Δz and interlayer distance Δr_{ij} for the PbSe (001) and (011) surfaces.

as indicated in Figure 2b. From the PDOS of the Pb and Se atoms at the (011) surface of PbSe, we can see that these surface states come mostly from these partially bonded surface atoms. The apparent differences between the (001) and (011) surfaces might be accounted for by the different surface rumpling and relaxation as illustrated in Figure 3. The layer rumpling and interlayer distances are calculated according to the definitions given by Sattal.³⁶ The surface states at the PbSe (011) surface might be related to the rather large surface rumpling and relaxation, which is due to the fact that the Pb or Se atoms at the (011) surface have more than one unsaturated bond. A similar result is also obtained for the (111) surface without saturation (see Figure 2c). The positive effect of pseudo-hydrogen atoms on the passivation of PbSe's dangling bonds can be validated by investigating their effect on the PbSe (011) and (111) surfaces. We can clearly see from Figure 2c that, after passivation, those surface states are eliminated and eventually the band gap is enlarged. For the (111) surface modeled in our calculation, the size effect is strong and we get an even larger band gap accordingly.

C. Rock-Salt PbSe Quantum Dots. 1. Structural Properties. Figure 4 gives the calculated atomic structures for bare and passivated PbSe QD $Pb_{14}Se_{13}$ (diameter $d = 11.216 \text{ \AA}$) before and after relaxation. As clearly illustrated in Figure 4, after relaxation, the bond length and bond angles of Pb–Se for *bare* QDs are significantly deviated from the unrelaxed one, which is nearly the same as those in bulk PbSe. However, in the presence of passivation, the distortions compared with relaxed bare ones are much smaller. The same phenomenon about stoichiometric PbSe QDs has also been observed by Franceschetti.^{16,38} Such large bond length deviation is also observed in the case of the PbTe (001) surface, where it is accounted for by surface relaxation and rumpling.^{36,39} We expect that this structural relaxation for surface atoms in “nonstoichiometric” PbSe QDs might be the reason for the existence of surface states inside the band gap as discussed below.

2. Density of States. For bare PbSe QDs, there are both Pb and Se dangling bonds at the surface. Figure 5 gives the DOS comparisons for QD $Pb_{14}Se_{13}$ after different surface disposals. The PDOSs of the unsaturated Pb and Se atoms at the surface are also given. We can see from Figure 5c,d that these unsaturated bonds introduce a large density of states inside the band gap, resulting in the reduction of its effective band gap. Furthermore, these in-gap states will influence the PL intensity significantly. As it is Se 6p electrons that participate in the

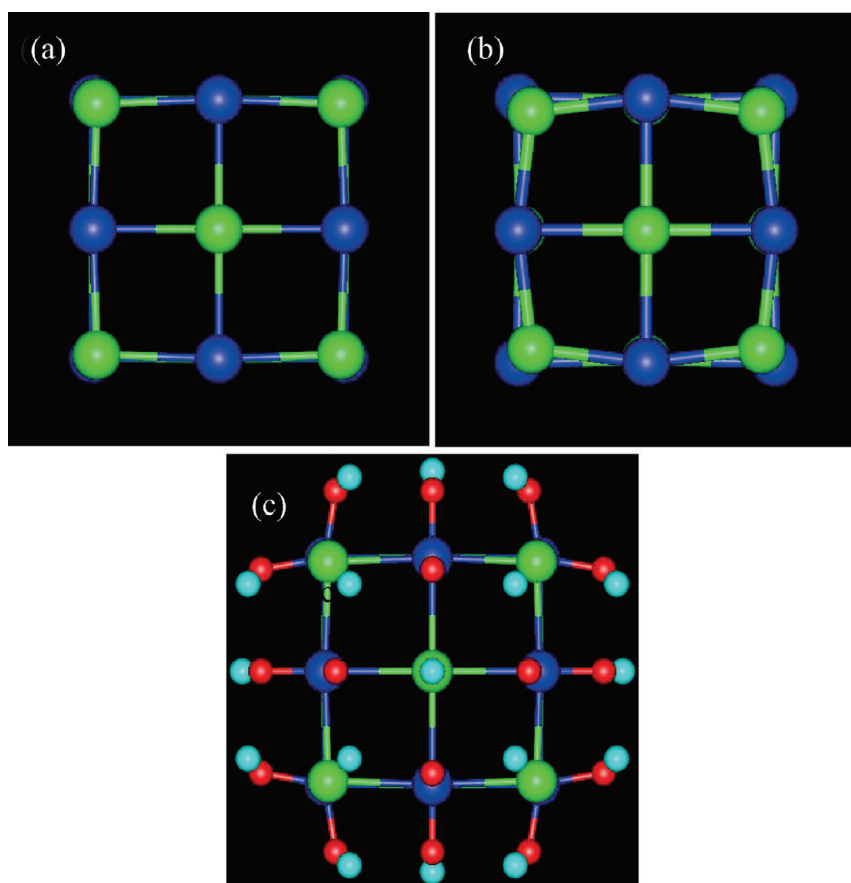


Figure 4. Atomic structures of PbSe QD1: unrelaxed bare QD (a), relaxed bare QD (b), and passivated QD (c). The green, blue, red, and sky-blue balls represent Pb, Se, ^{53}H , and $^{1\text{H}}$ atoms, respectively.

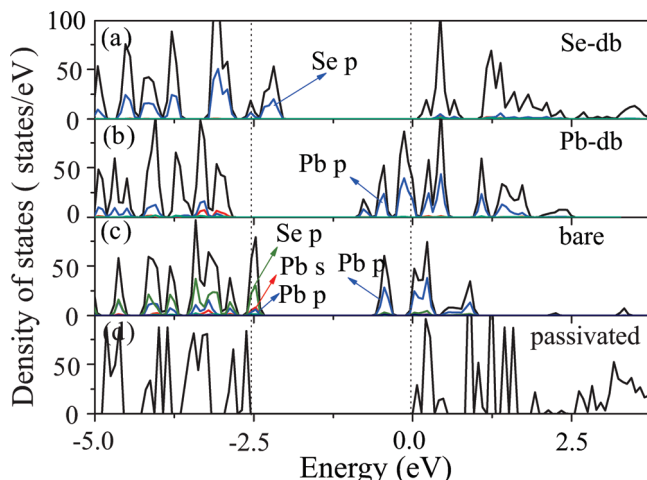


Figure 5. DOS for QD $\text{Pb}_{14}\text{Se}_{13}$: with Se dangling bonds (a), with Pb dangling bonds (b), with both Se and Pb dangling bonds (c), and fully passivated (d). The dotted lines indicate the band gap of the passivated QD.

bonding with Pb, the Se dangling bond induces a gap state above the VBM with Se p character (see Figure 5a). In the same way, the Pb dangling bond induces a gap state below the CBM with Pb p character (see Figure 5b). For the bare PbSe QD, the highest occupied states consist mainly of Pb p, Se p, and Pb s character, while the lowest unoccupied states consist mostly of Pb p character. The behaviors of the dangling bonds on the QDs studied in our work are entirely different from those of the stoichiometric PbSe QDs investigated by Franceschetti. During the fabrication of PbSe QDs, one is not able to ensure their

stoichiometry; i.e., the components of PbSe QDs are most probably under Pb-rich or Se-rich conditions. Therefore, our models are more comparable with the practical experiments.²⁰ And several experiments have proven the presence of surface states for PbSe QDs and the positive effect of surface dispositions on their optical properties.

3. Charge Densities. In Figures 6 and 7, we show the contour plots of charge density distributions for the highest occupied molecular orbital (HOMO) and lowest unoccupied molecular orbital (LUMO) states of the 21.452 Å PbSe QD before and after saturation with pseudo-hydrogen atoms. The contour plots are given from different viewing perspectives: from the left to the right in the [001], [011], and [111] directions, respectively. For the unsaturated QD illustrated in Figure 6, the HOMO and LUMO states have a significant weight at the edge of the QD. Looking closely at the HOMO states in Figure 6 (top), the orbital distributions appear to be on the Pb and Se atoms with dangling bonds, while the LUMO states appears to be centered on the Pb atoms at the surface. This is consistent with the PDOS plots for QD1 in Figure 5. For the saturated QD with the same numbers of Pb and Se atoms as in the unsaturated QD illustrated in Figure 7, we see that there is no surface state any more. The band edge states are distributed primarily in the interior of the QDs. This confirms that the pseudo-hydrogen passivation scheme also works well for the PbSe QDs.

4. Energy Gap. The size dependence of the band gaps is also studied for quantum dots containing up to 1153 atoms including the pseudo-hydrogen atoms. For QDs, the band gap is defined as the energy difference between the HOMO and LUMO states. Table 1 shows the LDA-calculated band gaps for the five spherical nonstoichiometric PbSe QDs. The quantum

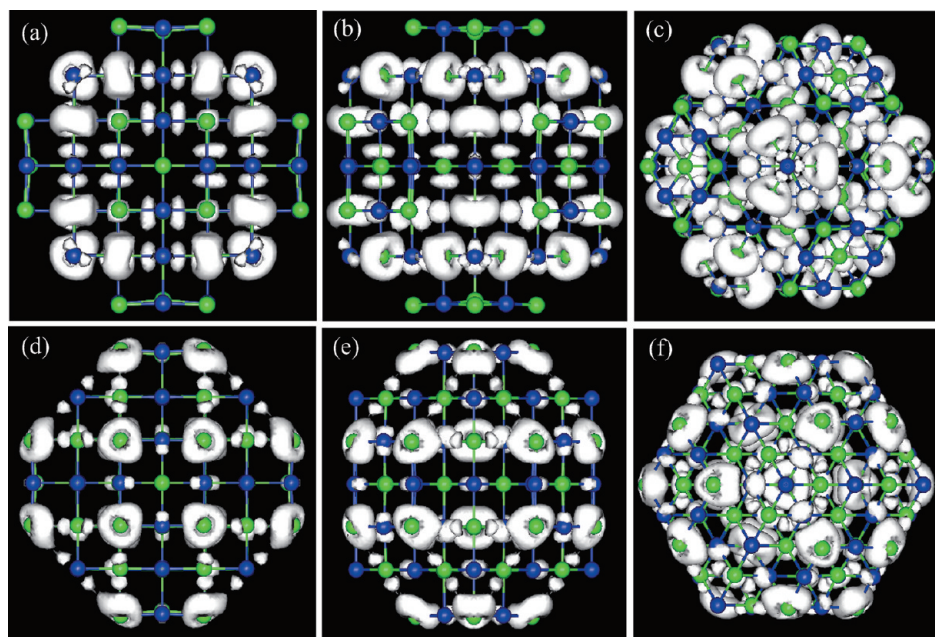


Figure 6. Wave function square contour plots of the HOMO state (top) and LUMO state (bottom) for the unpassivated PbSe QD $\text{Pb}_{92}\text{Se}_{97}$. (a) and (d), (b) and (e), and (c) and (f) are the views from the [001], [011], and [111] directions, respectively.

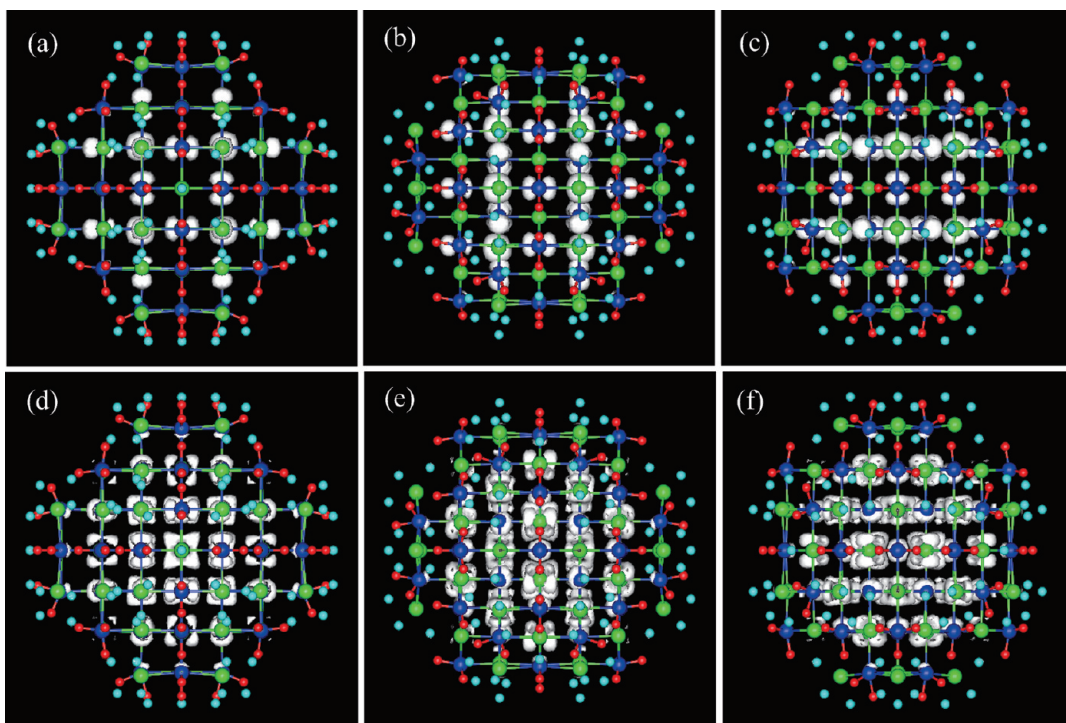


Figure 7. Same as in Figure 6, but for the passivated QD.

confinement energy, i.e., the relative band gap between the QDs and the bulk versus the effective size of the QDs is plotted in Figure 8 (black squares). To validate our results, we employed the screened hybrid functional proposed by Heyd et al.⁴⁰ (HSE03) to calculate the band shift for QD $\text{Pb}_{14}\text{Se}_{13}$. Such hybrid functionals have been very successful in giving the correct results for the electronic and structural properties of PbX ($X = \text{S}, \text{Se}$, and Te).⁴¹ As using the HSE method for the QDs with a large number of atoms is too expensive now, we chose the smallest QD $\text{Pb}_{14}\text{Se}_{13}$ in our calculations. The gap shift obtained from HSE03 is 2.667 eV, agreeing well with that from LDA (2.588 eV) as indicated in Figure 8. We fitted the relationship between ΔE_g and the effective diameter d of the QDs

according to the expression $\Delta E_g = \beta/d^\alpha$. The fitted curve is also given in Figure 8 (solid line), and here, we obtained $\alpha = 1.03$ for the PbSe QDs. This value is significantly smaller than the value of 2 obtained from the simple effective-mass model. The same trends compared from first-principles and effective-mass calculations are also obtained for II–VI, III–V, and IV semiconductors. The calculated α values from first principles for II–VI, III–V, and IV materials are about 1.2, 1.0, and 1.6, respectively.^{42,43} Surprisingly, our present value is in accordance with experimental measurement²⁰ and Allan's tight-binding calculations³² that ΔE_g varies mainly with $1/d$.

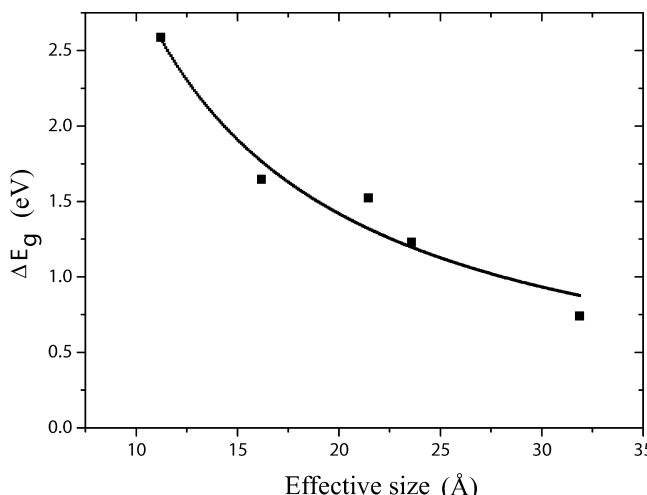


Figure 8. Change of the band gap ΔE_g as a function of the PbSe QD diameter d . The black squares and solid lines represent the calculated and the fitted values, respectively.

IV. Conclusions

In summary, the electronic properties of nonstoichiometric PbSe QDs are studied via the first-principles method. We find that unlike those at the stoichiometric QDs' surface, the dangling bonds at the nonstoichiometric QDs' surface induce states inside the band gap. These in-gap states introduced by the dangling Pb bonds exhibit the character of the Pb p state, while those from the dangling Se bonds have a character of the Se p state. The same trend is also observed for the unsaturated PbSe (011) and (111) surfaces, which is ascribed to the significantly large surface relaxation and rumpling. Pseudo-hydrogen atoms are employed to passivate these surface dangling bonds. This passivation scheme successfully removes the surface states from the energy gap. The HOMO and the LUMO states of the saturated quantum dots localize mostly in the interior of the dots, and they have atomic characteristics similar to those of the bulk PbSe. As the size decreases, the evolution of the band gap increases following the formula $\Delta E_g = 31.253/d^{1.032}$. The scaling rule of PbSe QDs obtained by first-principles calculations is in accordance with experiments and other theoretical calculations.

Acknowledgment. J.L. gratefully acknowledges financial support from the One-Hundred Talent Plan of the Chinese Academy of Sciences and National Science Fund for Distinguished Young Scholars (Grant No. 60925016). This work is supported by the National High Technology Research and Development program of China under Contract No. 2009AA034101.

References and Notes

- (1) *Semiconductors: Physics of Nontetrahedrally Bonded Binary Compounds II*; Landolt-Bornstein, Vol. III/17f; Springer-Verlag: Berlin, 1983.
- (2) Efros, A. L. *Sov. Phys. Semicond.* **1982**, *16*, 772.
- (3) Schaller, R. D.; Klimov, V. I. *Phys. Rev. Lett.* **2004**, *92*, 186601.
- (4) Isborn, C. M.; Prezhdo, O. V. *J. Phys. Chem. C* **2009**, *113*, 12617.
- (5) Isborn, C. M.; Kilina, S. V.; Li, X. S.; Prezhdo, O. V. *J. Phys. Chem. C* **2008**, *112*, 18291.
- (6) Kilina, S. V.; Craig, C. F.; Kilin, D. S.; Prezhdo, O. V. *J. Phys. Chem. C* **2007**, *111*, 4871.
- (7) Ellingson, R. J.; Beard, M. C.; Johnson, J. C.; Yu, P.; Micic, O. I.; Nozik, A. J.; Shabaev, A.; Efros, A. L. *Nano Lett.* **2005**, *5*, 865.
- (8) Kang, I.; Wise, F. W. *J. Opt. Soc. Am. B* **1997**, *14*, 1632.
- (9) Tudury, G. E.; Marquezini, M. V.; Ferreira, L. G.; Barbosa, L. C.; Cesari, C. L. *Phys. Rev. B* **2000**, *62*, 7357.
- (10) Allan, G.; Delerue, C. *Phys. Rev. B* **2004**, *70*, 245321.
- (11) Liljeroth, P.; Zeijlmans van Emmichoven, P. A.; Hickey, S. G.; Weller, H.; Grandidier, B.; Allan, G.; Vanmaekelbergh, D. *Phys. Rev. Lett.* **2005**, *95*, 086801.
- (12) An, J. M.; Dudy, S. V.; Franceschetti, A.; Zunger, A. *Nano Lett.* **2006**, *6*, 2728.
- (13) Ellingson, R. J.; Beard, M. C.; Johnson, J. C.; Yu, P.; Micic, O. I.; Nozik, A. J.; Shabaev, A.; Efros, A. L. *Nano Lett.* **2005**, *5*, 865.
- (14) Wehrenberg, B. L.; Wang, C.; Guyot-Sionnest, P. *J. Phys. Chem. B* **2002**, *106*, 10634.
- (15) Harbold, J. M.; Du, H.; Krauss, T. D.; Cho, K.-S.; Murray, C. B.; Wise, F. W. *Phys. Rev. B* **2005**, *72*, 195312.
- (16) Franceschetti, A. *Phys. Rev. B* **2008**, *78*, 075418.
- (17) Wang, L. W.; Zunger, A. *J. Phys. Chem.* **1994**, *98*, 2158.
- (18) Wang, L. W.; Li, J. *Phys. Rev. B* **2004**, *69*, 153302.
- (19) Li, J.; Wang, L. W. *Appl. Phys. Lett.* **2004**, *84*, 3648.
- (20) Moreels, I.; Lambert, K.; De Muynck, D.; Vanhaecke, F.; Poelman, D.; Martins, J. C.; Allan, G.; Hens, Z. *Chem. Mater.* **2007**, *19*, 6101.
- (21) Brumer, M.; Kigel, A.; Amirav, L.; Sashchiuk, A.; Solomesch, O.; Tessler, N.; Lifshitz, E. *Adv. Funct. Mater.* **2005**, *15*, 1111.
- (22) Sashchiuk, A.; Langof, L.; Chaim, R.; Lifshitz, E. *J. Cryst. Growth* **2002**, *240*, 431.
- (23) Wang, L. W.; Zunger, A. *Phys. Rev. B* **1995**, *51*, 17398.
- (24) Shiraishi, K. *J. Phys. Soc. Jpn.* **1990**, *59*, 3455.
- (25) Kresse, G.; Hafner, J. *Phys. Rev. B* **1993**, *47*, R558. 1993 48, 13115.
- (26) Blöchl, P. E. *Phys. Rev. B* **1994**, *50*, 17953. Kresse, G.; Joubert, J. *Phys. Rev. B* **1999**, *59*, 1758.
- (27) An, J. M.; Franceschetti, A.; Dudy, S. V.; Zunger, A. *Nano Lett.* **2006**, *6*, 2728.
- (28) Peng, H. W.; Li, J.; Li, S.-S.; Xia, J.-B. *J. Phys. Chem. C* **2008**, *112* (36), 13964.
- (29) Monkhorst, H. J.; Pack, J. D. *Phys. Rev. B* **1977**, *16*, 1748.
- (30) Wei, S.-H.; Krakauer, H. *Phys. Rev. Lett.* **1985**, *55*, 1200.
- (31) Wei, S.-H.; Zunger, A. *Phys. Rev. B* **1997**, *55*, 13605.
- (32) Allan, G.; Delerue, C. *Phys. Rev. B* **2004**, *70*, 245321.
- (33) *Semiconductors, II-VI and I-VII Compounds: Semimagnetic Compounds*; Rossler, U., Ed.; Landolt-Bornstein, New Series, Group III, Vol. 41; Springer-Verlag: Berlin, 2001.
- (34) Huang, X.; Lindgren, E.; Chelikowsky, R. *Phys. Rev. B* **2005**, *71*, 165328.
- (35) Allan, G. *Phys. Rev. B* **1991**, *43*, 9594.
- (36) Sattal, A.; de Gironcoli, S. *Phys. Rev. B* **200**, *63*, 033302.
- (37) Ma, J.; et al. *Surf. Sci.* **2004**, *551*, 91.
- (38) Franceschetti, A. *Phys. Rev. B* **2007**, *76*, 161301(R).
- (39) Lazarides, A. A.; Duke, C. B.; Paton, A.; Kahn, A. *Phys. Rev. B* **1995**, *52*, 14895.
- (40) Heyd, J.; Scuseria, G. E.; Ernzerhof, M. *J. Chem. Phys.* **2003**, *118*, 8207.
- (41) Hummer, K.; Grüneis, A.; Kresse, G. *Phys. Rev. B* **2007**, *75*, 195211.
- (42) Li, J.; Wang, L. W. *Chem. Mater.* **2004**, *16*, 4012.
- (43) Li, J.; Wang, L. W. *Phys. Rev. B* **2005**, *72*, 125325.